ORIGINAL RESEARCH

Biodegradable Flow Diverter for the Treatment of Intracranial Aneurysms: A Pilot Study Using a Rabbit Aneurysm Model

Hidehisa Nishi, MD; Akira Ishii, MD, PhD; Isao Ono, MD; Yu Abekura, MD; Hiroyuki Ikeda, MD, PhD; Daisuke Arai, MD, PhD; Yukihiro Yamao, MD, PhD; Masakazu Okawa, MD, PhD; Takayuki Kikuchi, MD, PhD; Akiyoshi Nakakura, MD; Susumu Miyamoto, MD, PhD

***Background*—**Herein, we report an in vivo study of a biodegradable flow diverter (BDFD) for aneurysm occlusion. Conceptually, BDFDs induce a temporal flow-diverting effect and provide a vascular scaffold for neointimal formation at the neck of the aneurysm until occlusion. This offers several potential advantages, including a reduced risk of remote ischemic complications and more treatment options in case of device failure to occlude the aneurysm.

***Methods and Results*—**A BDFD consisting of 48 poly-L-lactic acid wires with radiopaque markers at both ends was prepared. An in vitro degradation test of the BDFD was performed. Thirty-six BDFDs were implanted in a rabbit aneurysm model. Digital angiography, optical coherence tomography, histopathology, and scanning electron microscopy were performed after 1, 3, and 6 months, and 1 year. The in vitro degradation test showed that the BDFD was almost degraded in 1.5 years. In the in vivo experiment, aneurysm occlusion rates were 0% at 1 month, 20% at 3 months, 50% at 6 months, and 33% at 1 year. Optical coherence tomography showed that luminal area stenosis was the highest at 3 months (16%) and decreased afterward. Immunohistochemical analysis showed that more than half of the luminal surface area was covered by endothelial cells at 1 month. Device fragmentation was not observed in any lesions.

***Conclusions*—**This first in vivo study of a BDFD shows the feasibility of using BDFDs for treating aneurysms; however, a longer follow-up is required for comprehensive evaluation of the biological and mechanical behavior peculiar to biodegradable devices.
(*J Am Heart Assoc*. 2019;8:e014074. DOI: 10.1161/JAHA.119.014074.)

Key Words: aneurysm • biodegradable polymer • endovascular treatment • flow diverter • stent

The use of biodegradable vascular scaffolds has already been introduced in the field of interventional cardiology for the treatment of coronary artery disease in clinical settings. These scaffolds may potentially overcome the drawbacks of permanent coronary stents, such as late-stent thrombosis, late in-stent stenosis, and pathophysiological changes in the vessel wall caused by metallic caging of the artery.[1] However, the first-generation coronary biodegradable scaffolds were associated with a higher thrombosis rate compared with the standard drug-eluting stents, which is likely attributable to the large strut thickness.[2,3]

In the field of interventional neuroradiology, biodegradable polymers have been used in some detachable coils for aneurysm occlusion to enhance therapeutic efficacy. For example, poly (lactic-*co*-glycolic acid) has been used in the Matrix coil detachable system (Stryker, Minneapolis, MN), and poly (glycolic acid) has been used in the Cerecyte coil (DePuy Synthes, Raynham, MA). Polymer degradation was shown to increase tissue regeneration and cell proliferation response within the aneurysm sac, which is expected to decrease the aneurysm recanalization rate.[4,5]

Although some animal studies investigated the combined use of biodegradable polymers with metallic stents for intracranial use, no study investigated a device that fundamentally consisted of biodegradable materials intended for intracranial use.[6–8] Herein, we present the concept of a biodegradable flow diverter (BDFD), which provides a transient vascular scaffold for neointimal formation and induces a flow-diverting effect at the aneurysm neck. After the healing period, the degradation of the BDFD leaves the vessel with a healthy endothelium and normal vasomotion and renders it devoid of caging.

From the Departments of Neurosurgery (H.N., A.I., I.O., Y.A., H.I., D.A., Y.Y., M.O., T.K., S.M.) and Biomedical Statistics and Bioinformatics (A.N.), Kyoto University Graduate School of Medicine, Kyoto, Japan; Department of Neurosurgery, Fukui Red Cross Hospital, Fukui, Japan (H.I.); and Department of Neurosurgery, Shizuoka General Hospital, Shizuoka, Japan (D.A.).

Correspondence to: Hidehisa Nishi, MD, Department of Neurosurgery, Kyoto University Hospital, Sakyo-ku, Kyoto, Japan. E-mail: venturahighway83@gmail.com

Received July 25, 2019; accepted August 12, 2019.

Clinical Perspective

What Is New?

- We have introduced the treatment device concept of the "biodegradable flow diverters" for the cerebral aneurysms, which induce a temporal flow-diverting effect and provide a vascular scaffold for neointimal formation at the neck of the aneurysm until occlusion.
- The in vivo assessment showed that aneurysm occlusion is possible with these devices and displayed a certain feasibility of the device, especially on the preservation of the branching vessel and the extent of neointima formation.

What Are the Clinical Implications?

- Although they are in their initial stage of development, biodegradable flow diverters have potential to be a therapeutic option for cerebral aneurysms in the future.

The BDFD has several potential advantages against the metallic flow diverter (FD). Because the FD requires a high metal coverage rate for aneurysm occlusion, it is associated with a relatively high risk of ischemic complications. Remote ischemic events may occur >1 year after device placement.[9–11] Dual-antiplatelet therapy with aspirin and clopidogrel for 6 months after implantation is generally used to prevent late ischemic events, in return for the increased risk of hemorrhagic complications. The absence of residual foreign materials theoretically reduces the risk of late-stent thrombosis and in-stent stenosis; this may reduce the risk of remote ischemic complications. Besides, BDFDs will be more appropriate for pediatric patients and patients allergic to metals; in the event of treatment failure, there will be more options for salvage therapy after the BDFD absorption.

However, there are some concerns pertaining to biodegradable stent use in cerebral vessels. During degradation, biodegradable materials tend to induce a mild but persistent inflammatory response around the strut.[12,13] Whether the inflammation and consequent cell proliferation response during degradation are tolerable needs to be studied. In addition, because biodegradable polymers gradually lose their mechanical strength, the device may get deformed and fragmented during degradation.

Herein, we report a preclinical study of a BDFD for aneurysm treatment. Because this device is still in its early stage of development, we have focused on its feasibility, especially the biological response and morphometric changes in the parent vessel.

Materials and Methods

The data that support the findings of this study are available from the corresponding author on reasonable request.

BDFD Design

A high-molecular-weight poly-L-lactic acid polymer (weight-average molecular weight [Mw]=185 000 g/mol) was prepared. This polymer was processed into a thin fiber using a melt-spinning method until the strut thickness became 40 to 45 μm. Then, the poly-L-lactic acid fibers were woven into a braided structure composed of 48 fibers (Figure 1A and B). Annealing was performed by heating at 120°C for 2 hours. Three radiopaque gold markers were attached at both ends of the device. The designed size of the BDFD was 4.0×10, 4.0×12, and 4.0×15 mm. The BDFD was mounted onto a delivery system compatible with the 6F guiding catheter, and then the system was navigated to the vascular site with a 0.014-in guidewire. The BDFD was then pushed out from the delivery system with a delivery wire. Similar to the metallic braided stents, the BDFD undergoes self-expansion during deployment; however, it is not complete for its designed size. Routine angioplasty was performed after the deployment. The device is designed for degradation, except for the gold markers at both ends.

In Vitro Accelerated Degradation Test

To investigate the in vitro degradation, 10 samples of BDFD were placed in phosphate buffered saline (pH=7.4±0.2) at 70±1°C. On days 0, 3, 7, 10, 12, 14, 21, 28, 35, and 42, one sample was removed from the buffer, rinsed with distilled water, vacuum dried, and weighed. Then, each sample was subjected to gel permeation chromatography and differential scanning calorimetry.

The number-average molecular weight and Mw were measured using gel permeation chromatography. Gel permeation chromatography was performed at 40°C using a Shimadzu analyzer system. A Tosoh TSKgel SuperHZM-N column was used with chloroform as the eluent at a flow rate of 0.25 mL/min (Tosoh, Tokyo, Japan). A sample was injected at a concentration of 2.0 mg/mL. Polystyrene standards were used as the reference.

For the differential scanning calorimetry analysis, 2-mg samples were placed in sealed aluminum pans. The glass transition temperature, melting point of the fibers, and crystallinity were determined by increasing the temperature from 25°C to 220°C at 10°C/min using a thermoregulated differential scanning calorimeter (Bruker AXS, Billerica, MA).

In Vitro Real-Time Degradation Test

Twenty-four samples of the same polymer were placed in phosphate buffered saline (pH=7.4±0.2) at 37±1°C. On days 28 (n= 4), 91 (n=4), 182 (n=6), 273 (n=4), 364 (n=4), and 553 (n=2), number-average molecular weight and Mw were measured using gel permeation chromatography, similar to the accelerated degradation test.

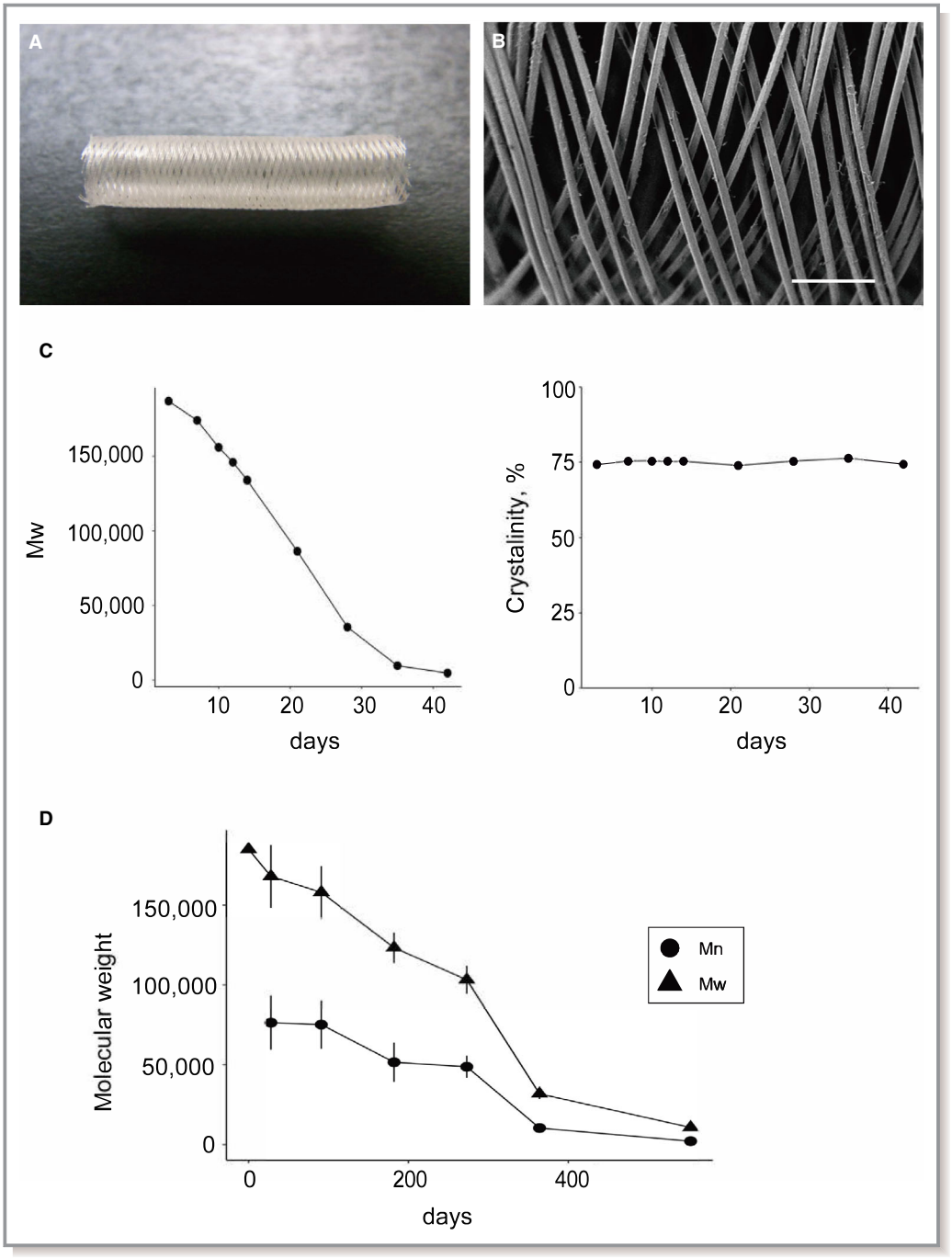

Figure 1. Scaffold design and in vitro evaluation. **A**, Photograph of the biodegradable flow diverter used in this study. **B**, A scanning electron microscopy image showing 40 to 45 μm braided wires composed of poly-L-lactic acid (bar=400 μm). **C**, Results of the accelerated degradation test showing a decrease in the weight-average molecular weight by 98% at 42 days. Throughout the degradation, crystallinity was maintained at ≈75%. **D**, Results of the real-time degradation test showing degradation of 95% of the device by 1.5 years. Mn indicates number-average molecular weight; Mw, weight-average molecular weight.

In Vivo Study Design and Animal Experiment

All experimental protocols were approved by the institutional animal care committee. Elastase-induced aneurysms were created in 18 female New Zealand white rabbits (weight, 2.6–3.0 kg).[14] Anesthesia was induced using an intravenous injection of pentobarbital and was maintained with 1% to 2% isoflurane throughout the procedure. Aneurysms were allowed to mature for at least 21 days before BDFD placement because the aneurysm is reported to mature 2 weeks after aneurysm creation.[14]

Animals were treated with aspirin (30 mg) for 5 days before BDFD placement. Through a right transfemoral approach, a 6F guiding catheter was placed into the right innominate artery. Subsequently, a microcatheter with a 0.014-in microguidewire was navigated into the subclavian artery distal to the aneurysm neck. The BDFD delivery system was advanced over the microguidewire using the exchange method. The wire was then removed, and BDFD was deployed across the aneurysm neck using a push-pull maneuver. After the deployment, balloon angioplasty with a 2.5- to 3.5-mm compliant balloon was performed within BDFD to achieve complete wall apposition of the device.

An additional BDFD was placed in the abdominal aorta across the origin of the lumbar artery using the same procedure. Subsequently, the guiding catheter and sheath were removed and the femoral artery was ligated and allowed to recover. The lumbar artery was used to assess the preservation capability of the intracranial stent with the small branching artery.[15–18]

Each animal was randomly allocated to the one of the specific time-point groups for the follow-up investigation: 1 month (n=5), 3 months (n=5), 6 months (n=5), and 1 year (n=3) after BDFD placement (Figure 2). After the procedure, antiplatelet therapy with aspirin (30 mg) was continued throughout the study duration.

Angiographic Analysis

After the observation period, follow-up angiography was performed and aneurysm occlusion was assessed using a 3-point scale (complete occlusion, neck remnant, and dome filling). The patency of the branch arteries covered by the device (including the left common carotid artery, right vertebral artery, and lumbar artery) was assessed using a binary scale (patent/occluded). To assess the downstream embolization, any occlusion or thrombus formation at the downstream arteries of the aneurysm, including the distal portion of the subclavian artery, internal mammary artery, brachial artery, and its small branches, was evaluated.

Optical Coherence Tomography

Optical coherence tomography (OCT) was performed using a commercially available frequency-domain OCT system (Lunawave; Terumo, Tokyo, Japan). Quantitative analyses were performed at 1-mm intervals within the device, which was defined as the region between the metallic radiopaque markers. Neointimal thickness was defined as the distance from the center of each strut to the luminal border. Quantitative area measurements in orthogonal angles were performed. The luminal and scaffold areas were drawn by a manual tracing method for each slice. The neointimal area was estimated as the scaffold area minus the luminal area. Luminal area stenosis was calculated by dividing the luminal area by the scaffold area. The appearance of the strut at each time point was visually assessed. Morphometric measurements were performed using the following equations:

$$\text{Neointimal area} = \text{scaffold area} - \text{luminal area},$$

$$\text{Luminal area stenosis} = 100 - (\text{luminal area}/\text{scaffold area}) \times 100.$$

Qualitative assessment was also performed at 1-mm intervals within the device for the presence of any mass protruding into the lumen, which reportedly is the sign of thrombosis formation at the luminal surface.[19] The thrombus within the aneurysm dome was excluded for this analysis. Red thrombus was defined by a protruding mass with high backscattering and attenuation, and white thrombus was defined by homogeneous backscattering and low attenuation, according to previous reports.[19] Thrombus formation was assessed using the following equation:

$$\text{Percentage thrombus formation} = (\text{number of thrombus positive sections}/\text{number of all sections}) \times 100.$$

Tissue Processing

After follow-up angiography and OCT, the animals were euthanized with a lethal dose of sodium pentobarbital and flushed with saline and 4% paraformaldehyde in phosphate buffered saline. Both the right subclavian artery and abdominal aorta were separately resected en bloc and placed directly in 4% paraformaldehyde in phosphate buffered saline solution for fixation. After overnight fixation, the samples were embedded in paraffin. Axial sections were prepared from the proximal, mid, and distal portions of the scaffold segment. For the subclavian artery, the midportion was set as the aneurysm site. A normal vessel was used as the control. The samples were cut axially at 5 μm using a low-speed saw.

Histopathological Analysis

Each sample was stained with hematoxylin and eosin and elastica–van Gieson stains. The tissues within the aneurysm dome were categorized as unorganized thrombus, organized thrombus, and collagenized connective tissue.[15] The vessel injury score was calculated using the Schwartz method.[20] This score has been used to assess vessel injury with the metallic FD.[15,16] Calculations were performed using the following equation:

$$\text{Mean injury score} = \text{sum of injury scores for each strutr}/\text{number of struts}.$$

All samples were immunostained by overnight incubation with primary antibodies against CD31 (1:20; Dako, Carpinteria,

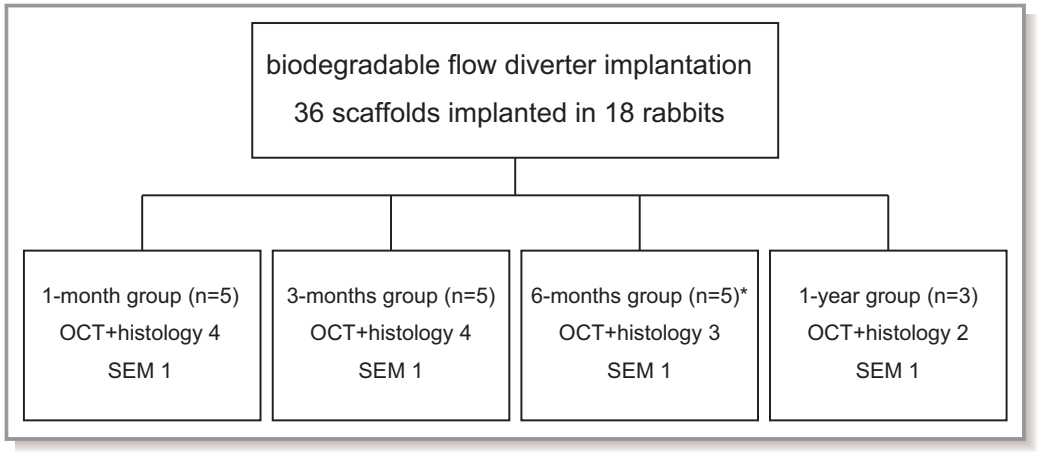

Figure 2. The experimental design of in vivo experiment. The biodegradable flow diverter (BDFD) was placed in the aneurysm model. Each animal was randomly allocated to one of the specific time-point groups for the follow-up investigation: 1 month (n=5), 3 months (n=5), 6 months (n=5), and 1 year (n=3) after BDFD placement. One animal in the 6-month group died from severe wound infection and was excluded from the analysis. OCT indicates optical coherence tomography; SEM, scanning electron microscopy.

CA), CD34 (1:500; GeneTex, Irvine, CA), smooth muscle actin (1:100; Novus, Centennial, CO), CD68 (1:100; Abcam, Cambridge, UK), and Ki-67 (1:100; Dako) at 4°C. Specific binding was visualized using a secondary antibody: Alexa 488 and 594 (Thermo Fisher Scientific, Waltham, MD). ProLong Gold antifade reagent with 4',6-diamidino-2-phenylindole (Thermo Fisher Scientific) was used as a nuclear counterstain. All images were obtained using a fluorescence microscope (BZ-X800; Keyence, Osaka, Japan). Whole slide imaging was performed for image analysis. All parts of the specimen were sequentially imaged at ×20 magnification; subsequently, the images were merged. After taking an image of the complete slide, the number of CD68- and Ki-67–positive cells within the neointima was counted. The extent of reendothelialization was defined as the percentage of the luminal circumference covered by CD31-positive cells after manual tracing. All imaging analyses were performed using a BZ-X800 analyzer (Keyence). The following equations were used for immunohistochemical analysis:

$$\text{Inflammation of the neointima} = \text{number of CD68-positive cells within the neointima},$$

$$\text{Neointimal cellular proliferation} = \text{number of Ki67-positive cells within the neointima},$$

$$\text{Re-endothelialization} = (\text{circumference of the CD31-positive portion of the lumen})/(\text{total luminal circumference}) \times 100.$$

Scanning Electron Microscopy

After follow-up angiography and OCT, one subject per each time point was used for scanning electron microscopy. The subject was first deeply anesthetized and then pressure perfused with saline, followed by a fixative solution of 4% paraformaldehyde. The samples were then harvested and fixed with 4% paraformaldehyde and 2% glutaraldehyde at 4°C overnight. After fixation, the arteries were incised at the long-axis direction of the vessel and gently opened to expose the aneurysm neck and the ostium of the lumbar artery. After fixation with 1% OsO_4 for 2 hours, the specimens were dehydrated, dried, and coated with a thin layer of platinum palladium. The specimens were then examined using a Hitachi S-4700 scanning electron microscope (Hitachi, Tokyo, Japan). Neointimal formation on the luminal surface, patency of the branching arteries, and occurrence of strut fragmentation were examined.

Statistical Analysis

Continuous variables are expressed as the mean±SD or median with interquartile range, depending on the distribution of the variable. The normality of distribution was assessed using a quantile-quantile plot and Shapiro-Wilk test.

Comparisons of the results of angiography, OCT, and histological examination over time were performed using a linear mixed effect model that evaluates the effect of time. Although the same animal was not evaluated at different time points, multiple short-axis measurements from the arterial segment were obtained with the OCT and histological analyses. Because a repeated assessment was performed for these analyses, the animal was specified as a random effect to account for the effects that individual animals might have on the results. When the distribution of the results was different from the normal distribution, the logarithm of the data was used. According to the relatively small sample size at each time point, the whole group was divided into 2 groups: the 1- to 3-month group was compared with the 6- to 12-month group. Two-sided P values of <0.05 were considered

statistically significant and expressed at 2 significance levels. All statistical analyses were performed using R statistical software (version 3.0.2) and SAS (version 9.4).

Results

All experimental procedures were successfully performed. After the experiment, one animal allocated to the 6-month follow-up group died because of a severe wound infection and was excluded from the analysis.

Polymer Degradation

The results are summarized in Figure 1. The initial Mw of the polymer was 185 000 g/mol. On real-time degradation analysis, we found a decrease in Mw of 15% at 91 days (3 months), 45% at 273 days (9 months), 83% at 364 days (1 year), and 95% at 553 days (1.5 years) (Figure 1D).

On accelerated degradation analysis, Mw decreased by 81% at 28 days and by 95% at 35 days. According to the differential scanning calorimetry analysis, the melting point decreased in accordance with the change in Mw: 187.5°C at 3 days, 183.4°C at 14 days, and 161.2°C at 42 days. Crystallinity was consistent throughout degradation: 74.2% at 3 days, 75.2% at 14 days, and 74.3% at 42 days (Figure 1C).

Angiographic Outcomes

The results are summarized in the Table and Figure 3. The location of the device was determined by the gold markers at both ends. The mean diameter of the parent artery was 2.9±0.5 mm. Aneurysm occlusion rates were 0% (0/5) at 1 month, 20% (1/5) at 3 months, 50% (2/4) at 6 months, and 33% (1/3) at 1 year. All branching arteries (4 left common carotid arteries, 3 vertebral arteries, and 17 lumbar arteries) were found patent at all time points (24/24, 100%). There was no downstream arterial occlusion or thrombus formation at the downstream arteries of the aneurysm.

Table. Morphometric Measurements at Various Time Points

Variable	1 mo (n=5)	3 mo (n=5)	6 mo (n=4)	1 y (n=3)
Aneurysm morphology, mean±SD, mm				
Height	3.6±1.0	5.6±1.5	5.8±2.1	5.3±1.3
Width	1.8±0.8	2.5±1.2	2.4±0.5	3.2±1.1
Neck	2.3±0.6	2.6±1.3	3.6±0.7	3.9±1.6
Aneurysm occlusion, n/total (%)				
Complete occlusion	0/5 (0)	1/5 (20)	2/4 (50)	1/3 (33)
Neck remnant	3/5 (60)	2/5 (40)	2/4 (50)	0/3 (0)
Branching artery patency, n/total (%)				
CCA	1/1 (100)	2/2 (100)	0/0 (N/A)	1/1 (100)
VA	2/2 (100)	1/1 (100)	0/0 (N/A)	0/0 (N/A)
Lumbar artery	5/5 (100)	5/5 (100)	4/4 (100)	3/3 (100)

CCA indicates common carotid artery; N/A, not available; VA, vertebral artery.

OCT Outcomes

The results are summarized in Figure 4. The location of BDFD was determined by the gold markers at both ends in all cases. Neointimal thickness was 70 μm (IQR, 60–90 μm) at 1 month, 90 μm (IQR, 60–120 μm) at 3 months, 80 μm (IQR, 60–100 μm) at 6 months, and 60 μm (IQR, 40–80 μm) at 1 year after BDFD placement. The luminal area stenosis was 13.4% (IQR, 11.2%–16.3%) at 1 month, 16.1% (IQR, 13.1%–19.0%) at 3 months, 11.8% (IQR, 10.3%–13.5%) at 6 months, and 11.4% (IQR, 10.2%–13.3%) at 1 year. The luminal area stenosis was significantly smaller for the 6- to 12-month group than the 1- to 3-month group (P=0.01). Because of the little strut thickness, no visible changes in the strut's appearance attributable to polymer degradation were apparent throughout the study. The percentage thrombus formation was 1.9%, 1.8%, 0.0%, and 0.0% at 1, 3, and 6 months and 1 year, respectively. All detected thrombi were relatively small white thrombi, and there was no thrombus at the ostia of the branching vessel.

Histopathological Outcomes

Among the occluded aneurysms, 1 was filled with a fresh thrombus, and the other 2 were filled with a fresh thrombus and organized tissue (Figure 3). The remaining 1 was used for scanning electron microscopy analysis and was not subjected to histological examination. The mean vessel injury scores were 0.09±0.20 at 1 month, 0.05±0.10 at 3 months, 0.09±0.19 at 6 months, and 0.03±0.05 at 1 year after BDFD placement; there was no significant difference between the 1- to 3-month and the 6- to 12-month groups in this respect (P=0.93).

The mean number of CD68-positive cells within the neointima was 31.5 (IQR, 8.25–78.75) at 1 month, 41.0 (IQR, 13.6–72.5) at 3 months, 22.5 (IQR, 14.7–58.2) at 6 months, and 9.5 (IQR, 6.25–20.5) at 1 year. Although the inflammatory response seemed to decrease over time after BDFD placement, there was no statistically significant difference between the 1- to 3-month and the 6- to 12-month groups (P=0.24). The number of Ki-67–positive cells within the neointima was 127.5 (IQR, 65.0–328) at 1 month, 86.5 (IQR, 43.2–273.2) at 3 months, 30.0 (IQR, 12.5–139.5) at 6 months, and 27.0 (IQR, 10–69.7) at 1 year. Cell proliferation decreased from the 1- to 3-month group to the 6- to 12-month group (P=0.03). The extent of neointimal reendothelialization was 63.0% (IQR, 43.5%–78.3%) at 1 month, 61.1%

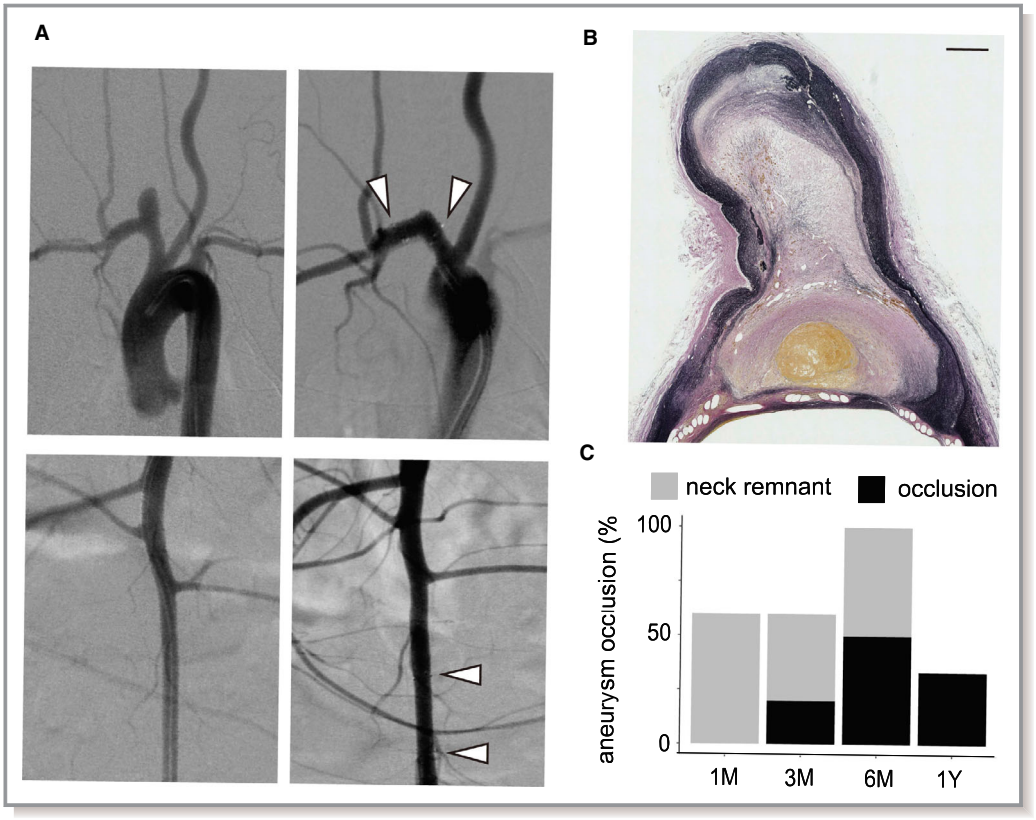

Figure 3. Representative images of the occluded aneurysm. **A**, Angiographic images of the aneurysm and the lumbar artery are shown. The first column displays the images before the implantation of the device, and the second column displays the images after the implantation of the device. The white arrowhead indicates the position of the gold marker. **B**, Elastica–van Gieson staining of the aneurysm showing a fresh thrombus and organized tissue within the aneurysm dome (bar=500 μm). **C**, Aneurysm occlusion profile at each time point.

(IQR, 55.8%–78.3%) at 3 months, 59.7% (IQR, 45.4%–67.7%) at 6 months, and 53.8% (IQR, 22.9%–69.3%) at 1 year. There was no significant difference in reendothelialization extent between the 1- to 3-month and the 6- to 12-month groups (P=0.45). No CD34-positive cells were observed throughout the experimental period. Immunohistochemistry results are summarized in Figure 5.

All branching arteries covered by BDFD were patent, including the left common carotid, vertebral, and lumbar arteries. No thrombus formed at the branching vessels and at the struts covering the branches. The struts covering these arteries were already surrounded by the neointima tissue at 1 month and made multiple tissue islands. At 1 to 3 months, several macrophages were detected around the struts, and these became rare after 6 months.

The neointima tissue consisted mainly of smooth muscle actin–positive myointimal cells, fibroblasts, and extracellular matrix with elastic and collagen fibers. In addition, the surface of the neointima was covered by the CD31-positive endothelial cells, although the reendothelialization was not complete. At 1 to 3 months, the CD68-positive macrophages surrounded the struts and became rare thereafter. There was no eosinophil infiltration or foreign body giant cell within the neointima. Although the myointimal cell layer seemed to not change, the fibroblasts gradually decreased, leaving the collagen fibers.

Scanning Electron Microscopy Findings

The appearance of the internal surface is shown in Figure 6. At 1 month, most struts were covered by the neointima. In addition, several scattered thrombi were observed on the surface. The thrombi became discreet and gradually reduced over time. We found no apparent strut fracture or fragmentation at the aneurysm ostia and branching vessels.

Discussion

To our knowledge, we have reported a device that represents the concept of a BDFD for the first time. Although it is in the early stages of development, the BDFD targets the cerebral aneurysms with anterior circulation, especially the internal carotid artery aneurysms.

In this study, the BDFD almost completely degraded, except for the radiopaque markers at both ends of the device. According to the in vitro degradation test, the BDFD

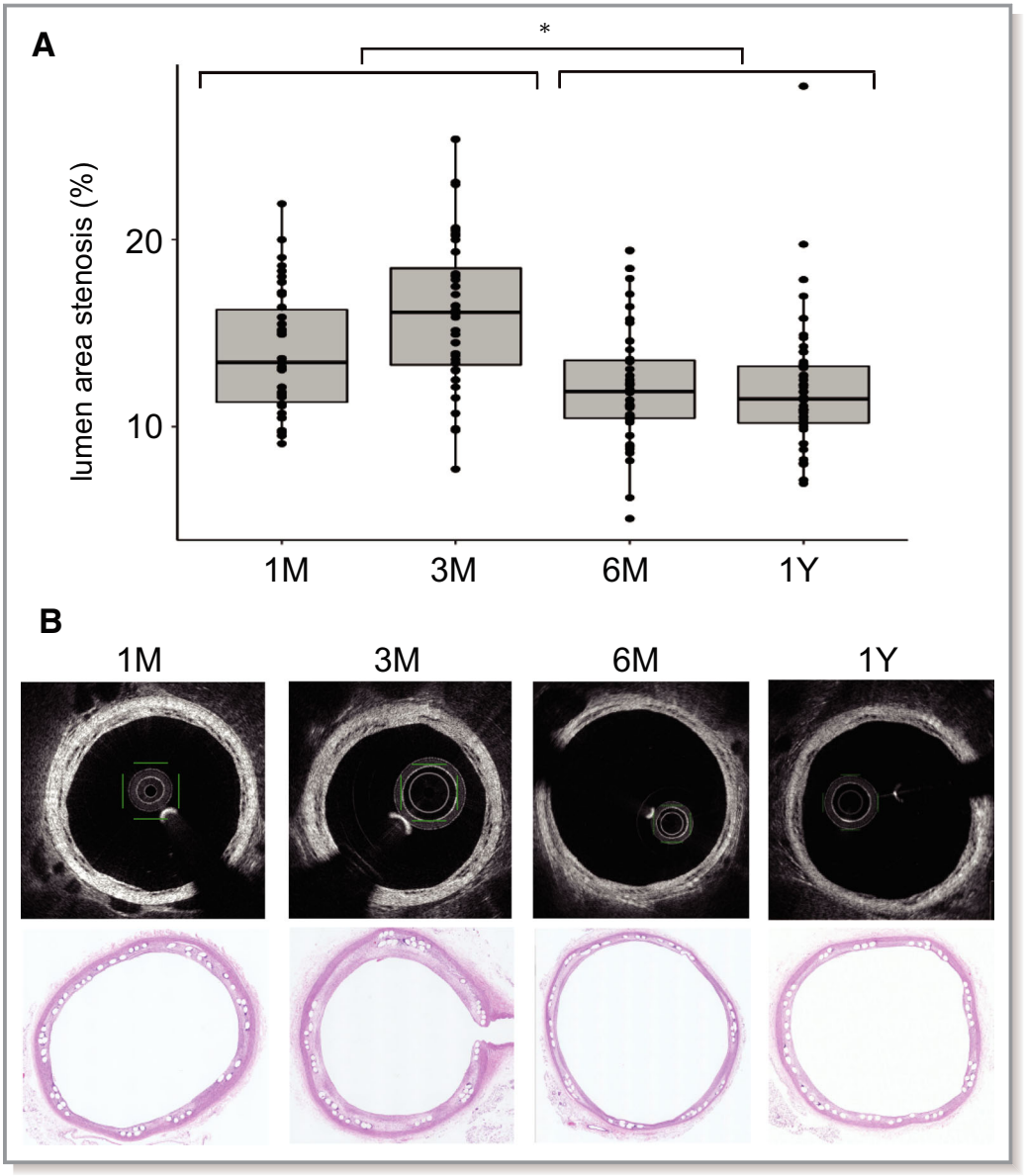

Figure 4. Optical coherence tomography (OCT) images showing luminal area stenosis of the parent artery at each time point. Each box plot shows the median, the quartiles, and the range. Each dot represents the lumen area stenosis at each section of the vessel. **A**, The stenosis rate at 1 to 3 months after implantation was higher than that at 6 to 12 months after implantation (linear mixed effect model). **B**, Representative images of OCT and hematoxylin and eosin staining. *P<0.05.

completely degrades at 1.5 years. Because the biodegradable polymer displays similar degradation behavior in vivo and in vitro, it is assumed that the BDFD will completely degrade at 1.5 years in vivo.[21]

We chose poly-L-lactic acid as the device material because of its biocompatibility, comparatively higher strength and stiffness, and slower absorption rate compared with other polymers.[22] Because of these desirable features, poly-L-lactic acid is the most commonly used platform for biodegradable scaffolds.

The main difference between our device and the currently used coronary biodegradable scaffolds is the strut thickness; although our device had a strut thickness of 40 μm, most coronary biodegradable scaffolds have a strut thickness of >100 μm. We could reduce the strut thickness because a much less radial force is required for intracranial aneurysms compared with the coronary biodegradable scaffold.[23] This is important because the current coronary biodegradable scaffolds failed to match the clinical results of standard metallic stents because of the higher

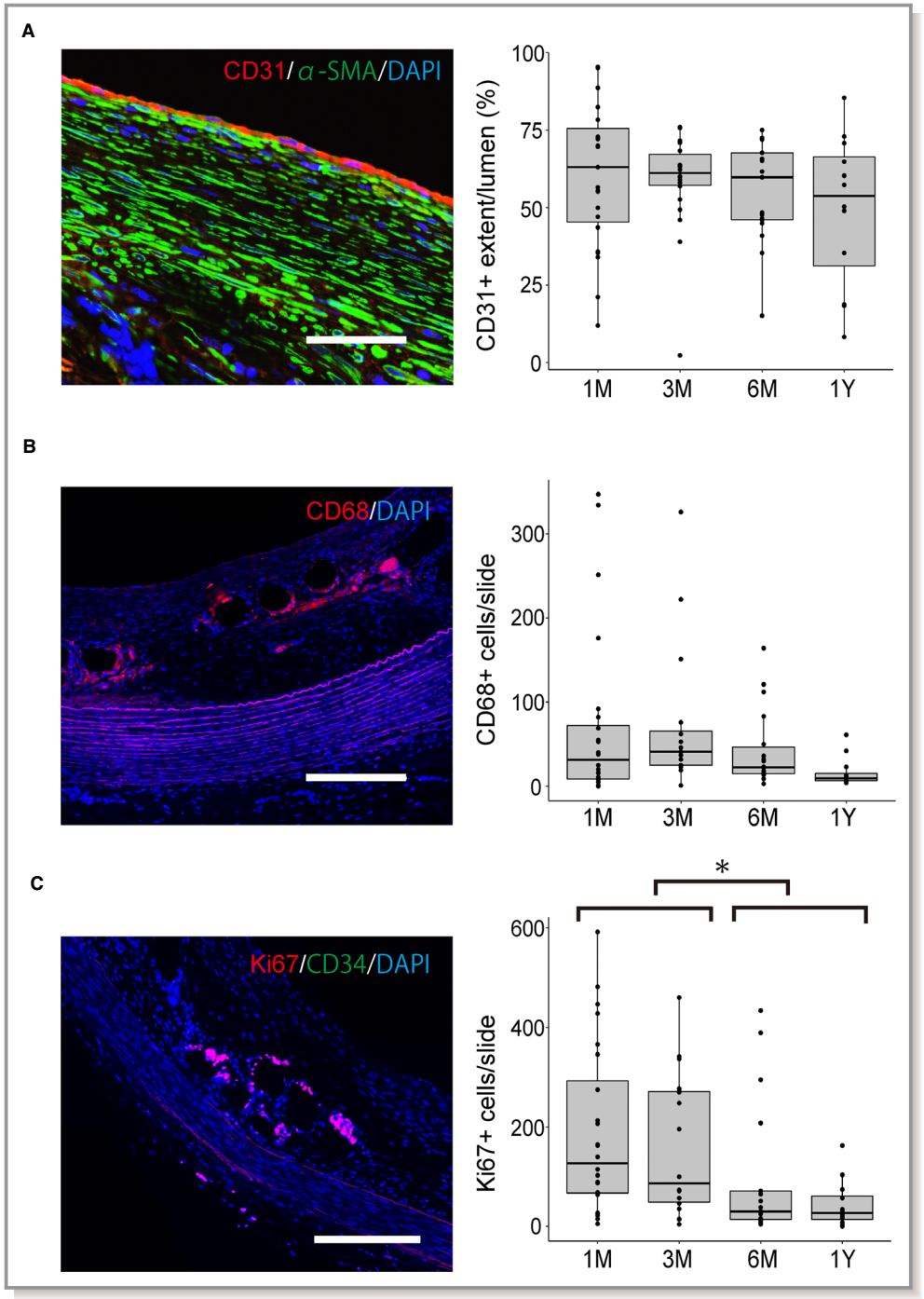

Figure 5. Histopathological analysis of the biological response after biodegradable flow diverter placement. Each dot represents the data per each slide. **A**, No significant difference was observed in reendothelialization at various time points. **B**, Although the inflammatory response seemed to decrease over time, the difference was not statistically significant (P=0.24). **C**, Cell proliferation at 1 to 3 months after implantation is greater than that at 6 to 12 months after implantation (linear mixed effect model). The box plots show the median, the quartiles, and the range (bar=200 μm). DAPI indicates 4',6-diamidino-2-phenylindole; α-SMA, α-smooth muscle actin. *P<0.05.

thrombosis rate attributable to the greater strut thickness.[2,3]

Although we avoided potential problems associated with excessive strut thickness, there were several concerns during the polymer-based FD development. In a previous coronary intervention study, biodegradable polymeric stents induced more prominent neointimal formation and a greater inflammatory response than metallic stents did, which persisted for

>3 years.[24] The present study focused on investigating the feasibility of this device.

The vessel morphological characteristics were assessed mainly using OCT. Contrary to our apprehensions, morphological results after device placement were similar to those achieved with a standard FD. Kallmes et al[15,16] performed animal experiments with first- and second-generation pipeline embolization devices. The reported injury score was 0.0 to 0.3, the neointima thickness was 100 to 200 μm, and the area stenosis was 8% to 20%. Our results are within the range of their results. In addition, similar temporal morphological changes of the neointima were observed in that the neointima formation peaked after 3 months.[15] Although this study was performed under single antiplatelet therapy, thrombus formation at the BDFD surface was rare, and no thrombus was detected after 6 months. Matsuda et al[19] reported that the metallic FD (Pipeline Flex) under single antiplatelet therapy displayed extensive thrombus formation at 7 days after device placement. Conversely, Marosfoi et al[25] reported no significant difference in the degree of acute thrombus formation between single or dual antiplatelet therapy, but there was a significant difference between the standard FD and the FD with phosphorylcholine coating. To the best of our knowledge, there is no report on thrombus formation with metallic FDs at the late time period, and direct comparison is required to assess whether there is a difference between metallic FDs and those with biodegradable polymers.

The biological response of the vessel wall was assessed using histological analyses. On the basis of the immunohistochemical analysis of Ki-67, although the implantation of the device induced some neointimal proliferation at 1 to 3 months, these responses attenuated after 6 months. This result was compatible with the OCT findings, which showed that lumen area stenosis decreased after 6 months. On the other hand, the number of CD68-positive cells was not significantly different from 1 to 3 months to 6 to 12 months, although there was a slight tendency to decrease. There are several studies that suggest a mild but persistent inflammatory response around the strut of the biodegradable vascular scaffold during degradation.[12,13,24] Because we did not perform a direct comparison with a metallic FD, we were unable to estimate the degree of the inflammatory responses of this device as excessive or not. But we were able to surmise that the persistent inflammation of the device did not result in the excessive neointima proliferation. The neointima tissue consisted mainly of myointima cells (smooth muscle cells) and extracellular matrix, covered by endothelial cells. These histological findings until 1 year were consistent with those of previous reports on the biodegradable scaffold in the cardiovascular literature.[26] Kadirvel et al[27] reported the histological findings after metallic FD placement and found that the neointima consisted mainly of smooth muscle actin–positive smooth muscle cells and the CD31-positive cells covering them. They also reported that the macrophages and

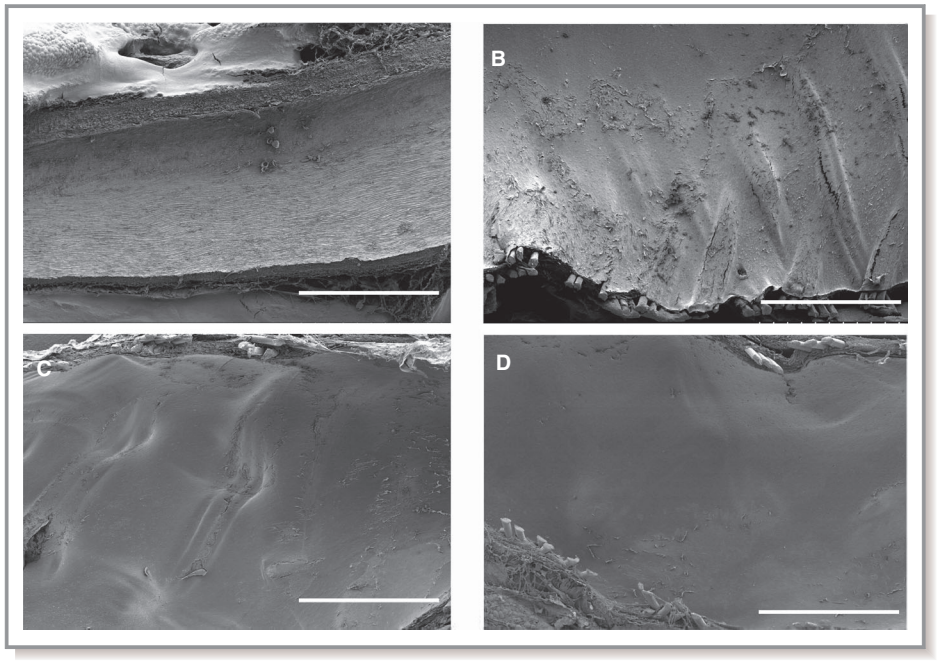

Figure 6. Scanning electron microscopy images of the vessel lumen. **A**, Normal abdominal aorta. **B**, Scaffold surface of the abdominal aorta. Some surface thrombi are observed at 1 month after biodegradable flow diverter implantation. **C**, No thrombi were observed at 6 months. **D**, The surface was smoother at 1 year (bar=1 mm).

monocytes were found at the struts covering the aneurysm neck.

Apart from the morphological and biological response, the major concern of the BDFD is the poor visibility under fluoroscope: only the 3 radiopaque markers at both ends are visible. Because the entire scaffold must be well opposed to the vessel wall, we performed angioplasty in every case to ensure wall apposition in this study.[28] To improve the radiopacity, the easiest way is to use the currently used biocompatible radiopaque wires, such as platinum-tungsten wires; in return, this will reduce the merit of the BDFD. Adding radiopaque compounds to the biodegradable polymer is another way, such as the Fantom Bioresorbable scaffold, which combined iodine and tyrosine-based polymer (REVA Medical, CA). Some sort of device improvement is strongly required in this aspect.

Finally, with respect to device performance, we found the occlusion rate at 6 months to be only 50%, which is lower than that previously reported with FDs (81%–99% at 6 months).[29] One reason for the low rate is that the device often displayed a relatively eccentric strut distribution after deployment, especially at the curved segment. The uneven distribution of the struts may have hindered the extension of the neointimal tissue at the aneurysm neck. Indeed, the device tested in this study was a first-generation prototype, and the scaffold design has since been modified with a designated 48-wire braider to improve strut distribution. Experiments are currently testing the efficacy of the newer prototype that exhibits a more even strut distribution. Apart from the device design, there is concern for aneurysm recanalization because the occlusion rate decreased by 50% at 6 months and by 33% at 1 year. Although this decline is merely caused by the relatively small sample size of this study, there is the possible mechanism of aneurysm recanalization inherent to BDFD. During the degradation process, BDFD gradually loses its mechanical strength. When the aneurysm is not completely occluded, this mechanical BDFD weakening can cause device deformation and fracture. Although we did not find any evidence of device fracture by OCT and histology, there remained the possibility of minor device deformation, such as minor strut movement or bending caused by the pulsatile blood flow. Because the tight mesh of the strut (low porosity and high pore density with even distribution) is reported to be an important factor for aneurysm occlusion, these possible minor BDFD deformations at the aneurysm neck can cause aneurysm recanalization, even if the device is not fractured.[30]

In clinical study, although >80% of aneurysms treated by FD achieve complete occlusion at 1 year, some aneurysms do occlude between 1 and 3 years.[10] If the aneurysm does not occlude at 1.5 years after BDFD placement, the aneurysm will have a high risk of recanalization and the risk of distal embolization of the thrombus formed within the dome of the aneurysm. These situations should be well investigated with preclinical studies, and the required duration of degradation with the weakening of the mechanical strength in mind must be well investigated.

Limitations

There are several limitations in this study. First, we did not set up a control group of untreated aneurysms or aneurysms treated with a permanent metallic FD. Untreated aneurysms were not assessed because the long-term patency of the elastase-induced rabbit aneurysm model has been previously established.[31] We did not include the current standard FD as a control because this device is a first-generation prototype and our primary focus was to assess device feasibility for the initial stage of development.

Second, although all branching arteries, including the carotid, vertebral, and lumbar arteries, were preserved in this study, concerns remain about the preservation of the intracranial perforating vessels. The median lumbar artery diameter was 248 μm in this study (IQR, 191–506 μm), and it was different from the intracranial perforating artery diameter, which reportedly ranges from 50 to 840 μm.[32] The preservation capability of the small arteries (<150 μm) was not tested in this study.

Third, the device requires improvements in several aspects. The tendency of eccentric strut distribution has already been resolved in our subsequent prototype, and we intend to assess the device's performance in another in vivo experiment. The radiopacity of the device is another important aspect, as discussed above, and we are investigating combination of biodegradable polymer and radiopaque materials.

Fourth, there is an undesirable mechanical behavior peculiar to polymeric materials, which was not mentioned in this study. Polymeric materials are frailer and more vulnerable to creep deformation than metals; this may cause a problem when the device is mounted on a narrow delivery system for a prolonged period. The self-expanding capacity decreases over time.[33]

Fifth, the full degradation period of BDFD was assessed only by the in vitro test. Although the degradation process is based mainly on the nonenzymatic hydrolysis in vivo and in vitro, the flow dynamics, mechanical stress from the vessel wall, and change in pH within the microenvironment also influence the degradation process.[34] The true degradation period should be evaluated with an in vivo model.

Last, although there was no evidence of device fragmentation and downstream arterial occlusion or thromboembolism, the tissue of the downstream territory was not assessed histologically for the microembolism. Fracture and fragmentation may occur later because of device weakening attributable

to biodegradation. There is a possibility of aneurysm recanalization along with device deformation and fracture, as discussed above; in addition, the fragmented element may cause cerebral infarction. These phenomena should be examined in preclinical studies with longer follow-ups.

Summary

This pilot study supports the concept of BDFDs for the treatment of saccular aneurysms. The analysis performed at the 1-year follow-up indicates device feasibility, especially of the morphological aspects. On the other hand, the inflammation response peculiar to the biodegradable scaffold should be further investigated. Our results also indicate the need to improve the device's design in several aspects, especially to increase the aneurysm occlusion capacity. The inherent risks associated with using biodegradable scaffolds were not fully elucidated in this study.

Acknowledgments

The authors would like to thank Kyoto Medical Planning (Kyoto, Japan) for its generous donation of the device and delivery system. The authors also would like to thank Dr T. Manabe of the Shiga General Hospital for the insightful comments and suggestions on the histopathological analysis.

Sources of Funding

This research is supported by The Translational Research Program; Strategic Promotion for Practical Application of Innovative Medical Technology from Japan Agency for Medical Research and Development.

Disclosures

None.

References

1. Ang HY, Bulluck H, Wong P, Venkatraman SS, Huang Y, Foin N. Bioresorbable stents: current and upcoming bioresorbable technologies. *Int J Cardiol*. 2017;228:931–939.
2. Cassese S, Byrne RA, Ndrepepa G, Kufner S, Wiebe J, Repp J, Schunkert H, Fusaro M, Kimura T, Kastrati A. Everolimus-eluting bioresorbable vascular scaffolds versus everolimus-eluting metallic stents: a meta-analysis of randomized controlled trials. *Lancet*. 2016;387:537–544.
3. Stone GW, Gao R, Kimura T, Kereiakes DJ, Ellis S, Onuma Y, Cheong WF, Jones-McMeans J, Su X, Zhang Z, Serruys PW. 1-Year outcomes with the Absorb bioresorbable scaffold in patients with coronary artery disease: a patient-level, pooled meta-analysis. *Lancet*. 2016;387:1277–1289.
4. Murayama Y, Vinuela F, Tateshima S, Gonzalez NR, Song JK, Mahdavieh H, Iruela-Arispe L. Cellular responses of bioabsorbable polymeric material and Guglielmi detachable coil in experimental aneurysms. *Stroke*. 2002;33:1120–1128.
5. Murayama Y, Tateshima S, Gonzalez NR, Vinuela F. Matrix and bioabsorbable polymeric coils accelerate healing of intracranial aneurysms: long-term experimental study. *Stroke*. 2003;34:2031–2037.
6. Schellhammer F, Berlis A, Bloss H, Pagenstecher A, Schumacher M. Poly-lactic-acid coating for endovascular stents: preliminary results in canine experimental arteriovenous fistulae. *Invest Radiol*. 1997;32:180–186.
7. Wang JB, Zhou B, Gu XL, Li MH, Gu BX, Wang W, Li YD. Treatment of a canine carotid artery aneurysm model with a biodegradable nanofiber-covered stent: a prospective pilot study. *Neurol India*. 2013;61:282–287.
8. Wang K, Yuan S, Zhang X, Liu Q, Zhong Q, Zhang R, Lu P, Li J. Biodegradable flow-diverting device for the treatment of intracranial aneurysm: short-term results of a rabbit experiment. *Neuroradiology*. 2013;55:621–628.
9. Fiorella D, Hsu D, Woo HH, Tarr RW, Nelson PK. Very late thrombosis of a pipeline embolization device construct: case report. *Neurosurgery*. 2010;67:onsE313–onsE314.
10. Becske T, Brinjikji W, Potts M, Kallmes DF, Shapiro M, Moran CJ, Levy EI, McDougall CG, Szikora I, Lanzino G, Woo HH, Lopes DK, Siddiqui AH, Albuquerque FC, Fiorella DJ, Saatci I, Cekirge SH, Berez AL, Cher DJ, Berentei Z, Marosfoi M, Nelson PK. Long-term clinical and angiographic outcomes following pipeline embolization device treatment of complex internal carotid artery aneurysms: five-year results of the pipeline for uncoilable of failed aneurysm trial. *Neurosurgery*. 2017;80:40–48.
11. Bhogal P, Ganslandt O, Bazner H, Henkes H, Perez MA. The fate of side branches covered by flow diverters: results from 140 patients. *World Neurosurg*. 2017;103:789–798.
12. Zamiri P, Kuang Y, Sharma U, Ng TF, Busold RH, Rago AP, Core LA, Palasis M. The biocompatibility of rapidly degrading polymeric stents in porcine carotid arteries. *Biomaterials*. 2010;31:7847–7855.
13. Durand E, Lemitre M, Couty L, Sharkawi T, Brasselet C, Vert M, Lafont A. Adjusting a polymer formulation for an optimal bioresorbable stent: a 6-month follow-up study. *EuroIntervention*. 2012;8:242–249.
14. Altes TA, Cloft HJ, Short JG, DeGast A, Do HM, Helm GA, Kallmes DF; American Roentgen Ray Society. 1999 ARRS Executive Council Award: creation of saccular aneurysms in the rabbit: a model suitable for testing endovascular devices. *AJR Am J Roentgenol*. 2000;174:349–354.
15. Kallmes DF, Ding YH, Dai D, Kadirvel R, Lewis DA, Cloft HJ. A new endoluminal, flow-disrupting device for treatment of saccular aneurysms. *Stroke*. 2007;38:2346–2352.
16. Kallmes DF, Ding YH, Dai D, Kadirvel R, Lewis DA, Cloft HJ. A second-generation, endoluminal, flow-disrupting device for treatment of saccular aneurysms. *AJNR Am J Neuroradiol*. 2009;30:1153–1158.
17. Masuo O, Terada T, Walker G, Tsuura M, Matsumoto H, Tohya K, Kimura M, Nakai K, Itakura T. Study of the patency of small arterial branches after stent placement with an experimental in vivo model. *AJNR Am J Neuroradiol*. 2002;23:706–710.
18. Masuo O, Terada T, Walker G, Tsuura M, Nakai K, Itakura T. Patency of perforating arteries after stent placement? A study using an in vivo experimental atherosclerosis-induced model. *AJNR Am J Neuroradiol*. 2005;26:543–548.
19. Matsuda Y, Jang DK, Chung J, Wainwright JM, Lopes D. Preliminary outcome of single antiplatelet therapy for surface-modified flow diverters in an animal model: analysis of neointimal development and thrombus formation using OCT. *J Neurointerv Surg*. 2019;11:74–79.
20. Schwartz RS, Huber KC, Murphy JG, Edwards WD, Camrud AR, Vlietstra RE, Holmes DR. Restenosis and the proportional neointimal response to coronary artery injury: results in a porcine model. *J Am Coll Cardiol*. 1992;19:267–274.
21. Weir NA, Buchanan FJ, Orr JF, Dickson GR. Degradation of poly-L-lactide, part 1: in vitro and in vivo physiological temperature degradation. *Proc Inst Mech Eng H*. 2004;218:307–319.
22. Shive MS, Anderson JM. Biodegradation and biocompatibility of PLA and PLGA microspheres. *Adv Drug Deliv Rev*. 1997;28:5–24.
23. Krischek O, Miloslavski E, Fischer S, Shrivastava S, Henkes H. A comparison of functional and physical properties of self-expanding intracranial stents. *Minim Invasive Neurosurg*. 2011;54:21–28.
24. Otsuka F, Pacheco E, Perkins LEL, Lane JP, Wang Q, Kamberi M, Frie M, Wang J, Sakakura K, Yahagi K, Ladich E, Rapoza RJ, Kolodgie FD, Virmani R. Long-term safety of an everolimus-eluting bioresorbable vascular scaffold and the cobalt-chromium XIENCE V stent in a porcine coronary artery model. *Circ Cardiovasc Interv*. 2014;7:330–342.
25. Marosfoi M, Clarencon F, Langen ET, King RM, Brooks OW, Tamura T, Wainwright JM, Gounis MJ, Vedantham S, Puri AS. Acute thrombus formation on phosphorilcholine surface modified flow diverters. *J Neurointerv Surg*. 2018;10:406–410.
26. Onuma Y, Serruys PW, Perkins LEL, Okamura T, Gonzalo N, Garcia-Garcia HM, Regar E, Kamberi M, Powers JC, Rapoza R, van Beusekom H, van der Giessen W, Virmani R. Intracoronary optical coherence tomography and histology at 1 month and 2, 3, and 4 years after implantation of everolimus-eluting bioresorbable vascular scaffolds in a porcine coronary artery model: an attempt to decipher the human optical coherence tomography images in the ABSORB trial. *Circulation*. 2010;122:2288–2300.

27. Kadirvel R, Ding YH, Dai D, Rezek I, Lewis DA, Kallmes DF. Cellular mechanisms of aneurysm occlusion after treatment with a flow diverter. *Radiology*. 2014;270:394–399.

28. Rouchaud A, Ramana C, Brinjikji W, Ding YH, Dai D, Gunderson T, Cebral J, Kallmes DF, Kadirvel R. Wall apposition is a key factor for aneurysm occlusion after flow diversion: a histologic evaluation in 41 rabbits. *AJNR Am J Neuroradiol*. 2016;37:2087–2091.

29. Fahed R, Raymond J, Ducroux C, Gentric JC, Salazkin I, Ziegler D, Gevry G, Darsaut TE. Testing flow diversion in animal models: a systematic review. *Neuroradiology*. 2016;58:375–382.

30. Sadasivan C, Cesar L, Seong J, Rakian A, Hao Q, Tio FO, Wakhloo AK, Lieber BB. An original flow diversion device for the treatment of intracranial aneurysms: evaluation in the rabbit elastase-induced model. *Stroke*. 2009;40:952–958.

31. Ding YH, Dai D, Lewis DA, Danielson MA, Kadirvel R, Cloft HJ, Kallmes DF. Long-term patency of elastase-induced aneurysm model in rabbits. *AJNR Am J Neuroradiol*. 2006;27:139–141.

32. Marinkovic SV, Milisavljevic MM, Kovacevic MS, Stevic ZD. Perforating branches of the middle cerebral artery: microanatomy and clinical significance of their intracerebral segments. *Stroke*. 1985;16:1022–1029.

33. Nuutinen JP, Clerc C, Reinikainen R, Tormala P. Mechanical properties and in vitro degradation of bioabsorbable self-expanding braided stents. *J Biomater Sci Polym Ed*. 2003;14:255–266.

34. Furukawa T, Matsue Y, Yasunaga T, Shikinami Y, Okuno M, Nakamura T. Biodegradation behavior of ultra-high-strength hydroxyapatite/poly (L-lactide) composite rods for internal fixation of bone fractures. *Biomaterials*. 2000;21:889–898.